Chronic β-Cell Depolarization Impairs β-Cell Identity by Disrupting a Network of Ca^{2+}-Regulated Genes

Jennifer S. Stancill,[1,2] Jean-Philippe Cartailler,[2] Hannah W. Clayton,[1,2] James T. O'Connor,[2] Matthew T. Dickerson,[3] Prasanna K. Dadi,[3] Anna B. Osipovich,[2,3] David A. Jacobson,[3] and Mark A. Magnuson[1,2,3]

Diabetes 2017;66:2175–2187 | https://doi.org/10.2337/db16-1355

We used mice lacking *Abcc8*, a key component of the β-cell K_{ATP}-channel, to analyze the effects of a sustained elevation in the intracellular Ca^{2+} concentration ($[Ca^{2+}]_i$) on β-cell identity and gene expression. Lineage tracing analysis revealed the conversion of β-cells lacking *Abcc8* into pancreatic polypeptide cells but not to α- or δ-cells. RNA-sequencing analysis of FACS-purified *Abcc8*$^{-/-}$ β-cells confirmed an increase in *Ppy* gene expression and revealed altered expression of more than 4,200 genes, many of which are involved in Ca^{2+} signaling, the maintenance of β-cell identity, and cell adhesion. The expression of *S100a6* and *S100a4*, two highly upregulated genes, is closely correlated with membrane depolarization, suggesting their use as markers for an increase in $[Ca^{2+}]_i$. Moreover, a bioinformatics analysis predicts that many of the dysregulated genes are regulated by common transcription factors, one of which, *Ascl1*, was confirmed to be directly controlled by Ca^{2+} influx in β-cells. Interestingly, among the upregulated genes is *Aldh1a3*, a putative marker of β-cell dedifferentiation, and other genes associated with β-cell failure. Taken together, our results suggest that chronically elevated β-cell $[Ca^{2+}]_i$ in *Abcc8*$^{-/-}$ islets contributes to the alteration of β-cell identity, islet cell numbers and morphology, and gene expression by disrupting a network of Ca^{2+}-regulated genes.

In type 2 diabetes (T2D), pancreatic β-cells fail to respond appropriately to metabolic stresses brought on by age, obesity, and genetic risk factors. The mechanisms by which chronic metabolic stress, including insulin resistance, glucotoxicity, and lipotoxicity (1–3), impair β-cell function are not understood. Although metabolic stress is usually considered to be exogenous to the β-cell, chronic stimulation leads to changes within the β-cell, impairing function. One such factor is chronic elevation in the concentration of intracellular Ca^{2+} ($[Ca^{2+}]_i$), sometimes called excitotoxicity (4), which may be triggered by sustained β-cell depolarization resulting from chronic stimulation.

Ca^{2+} is a ubiquitous second messenger that is central to regulating cellular dynamics of many cell types, including β-cells. Genetic and pharmacological perturbations that stimulate or impair Ca^{2+}signaling have dramatic effects on β-cell function. For instance, the disruption of calcineurin, a Ca^{2+}-dependent phosphatase, or Ca^{2+}/calmodulin-dependent protein kinase II or IV, two Ca^{2+}-dependent kinases, profoundly impairs β-cell function, likely by modulating the activity of Ca^{2+}-responsive transcription factors such as NFAT, CREB, and TORC2 (5–9). Conversely, the constitutive activation of calcineurin or calmodulin, a Ca^{2+} binding protein, also causes marked β-cell dysfunction (3,10,11).

Acutely, glucose metabolism induces ATP-sensitive potassium (K_{ATP}) channel closure, membrane depolarization, opening of voltage-gated Ca^{2+}channels, a rise in $[Ca^{2+}]_i$, and insulin secretion. However, sustained elevation in $[Ca^{2+}]_i$ has multiple effects on β-cell function that can be adaptive or maladaptive. β-Cell proliferation induced by glucose metabolism (12) is an example of an adaptive response to sustained elevations in $[Ca^{2+}]_i$. However, chronically elevated $[Ca^{2+}]_i$ can also induce maladaptive responses because prevention of Ca^{2+} influx in the setting of insulin resistance prevents β-cell death (13). In either case, mice lacking K_{ATP} channels exhibit disrupted islet morphology, characterized by α-cells being located in the islet core (14,15), suggesting loss of β-cell identity or impairments in cell adhesion.

[1]Department of Cell and Developmental Biology, Vanderbilt University, Nashville, TN
[2]Center for Stem Cell Biology, Vanderbilt University, Nashville, TN
[3]Department of Molecular Physiology and Biophysics, Vanderbilt University, Nashville, TN

Corresponding author: Mark A. Magnuson, mark.magnuson@vanderbilt.edu.

Received 7 November 2016 and accepted 17 May 2017.

This article contains Supplementary Data online at http://diabetes.diabetesjournals.org/lookup/suppl/doi:10.2337/db16-1355/-/DC1.

Here, we show that β-cells in *Abcc8*$^{-/-}$ mice exhibit chronic membrane depolarization and a sustained elevation in $[Ca^{2+}]_i$ and dysregulation of more than 4,200 genes, many of which are involved in cell adhesion, Ca^{2+}binding and Ca^{2+}signaling, and maintenance of β-cell identity. We also report that *Abcc8*$^{-/-}$ mice exhibit β-cell to pancreatic polypeptide (PP)–cell *trans*-differentiation and have increased expression of *Aldh1a3,* a gene recently suggested as a marker of dedifferentiating β-cells. In addition, we show that *S100a6* and *S100a4*, two EF-hand Ca^{2+} binding proteins, are acutely regulated in β-cells by membrane depolarization agents, suggesting that they may be markers for β-cell excitotoxicity. Finally, we performed a computational analysis to predict components of the gene regulatory network that may govern the observed gene expression changes and found that one of the predicted regulators, *Ascl1*, is directly regulated by Ca^{2+} influx in β-cells.

RESEARCH DESIGN AND METHODS

Mouse Lines

All animal experimentation was approved by the Vanderbilt Institutional Animal Care and Use Committee. *Abcc8*$^{-/-}$ (*Abcc8*$^{tm1.1Mgn}$, MGI: 2388392), *RIP-Cre* (*Tg.Ins2-cre*^{25Mgn}, MGI: 2176227), and *R26*$^{LSL.YFP}$ (*Gt [ROSA]26Sor*$^{tm[EYFP]Cos}$, MGI: 2449038) mice were congenic C57BL/6 and genotyped as previously described (16–18). *MIP-GFP* mice (*Tg [Ins1-EGFP/GH1]*^{14Hara}, MGI: 3583654) were congenic CD-1 and genotyped as previously described (19).

Glucose Tolerance Testing

After a 16-h fast, male *Abcc8*$^{+/+}$ and *Abcc8*$^{-/-}$ C57BL/6 mice were given intraperitoneal injection of D-glucose (2 mg/g body weight). Blood glucose was measured using a BD Logic glucometer.

Verapamil Administration

Adult *Abcc8*$^{+/+}$*;MIP-GFP* and *Abcc8*$^{-/-}$*;MIP-GFP* mice were given Splenda (2%) or a combination of verapamil (1 mg/mL; Sigma-Aldrich, V4629) and Splenda in their drinking water for 3 weeks. Splenda was used to mask the taste of verapamil.

Immunofluorescence Microscopy

Pancreata were fixed in 4% paraformaldehyde, frozen, and sectioned at a depth of 8 μm. Immunofluorescence staining was performed as previously described (20). Antibodies are listed in the Supplementary Data. Images were acquired using an Olympus FV-1000 confocal microscope, pseudocolored using ImageJ, and are representative of the phenotype observed in at least three animals. Cell death was determined using the *In Situ* Cell Death Detection Kit (Roche, 11684795910).

Islet Isolation

Pancreata were injected with 0.6 mg/mL collagenase P (Roche, 11213865001) into the pancreatic bile duct. Dissociated tissue was fractionated using Histopaque-1077 (Sigma-Aldrich, 10771), followed by hand-picking of islets. For FACS and RNA sequencing (RNA-Seq), islets from four to seven mice were pooled per sample. For quantitative RT-PCR (qRT-PCR), islets from a single mouse were used per sample.

Resting Membrane Potential

Islets were isolated from pancreata of 7- to 10-week-old *Abcc8*$^{+/+}$*;MIP-GFP* and *Abcc8*$^{-/-}$*;MIP-GFP* mice, and electrophysiological recordings were performed as previously described (21).

Ca^{2+} Imaging

Islets were isolated from pancreata of 9- to 11-week-old *Abcc8*$^{+/+}$and *Abcc8*$^{-/-}$ mice, and imaging of cytoplasmic Ca was performed as previously described (22).

Islet Culture

Wild-type islets were incubated for 24 h in DMEM (Gibco, 11966-025) containing 5.6 mmol/L glucose, 10% FBS (Gibco, 16140–071), and 1% penicillin-streptomycin (Gibco, 15140-122). Experimental media contained 100 μmol/L tolbutamide (Sigma-Aldrich, T0891) or 20 mmol/L KCl (Sigma-Aldrich, P5405), with or without 50 μmol/L verapamil.

Cell Isolation

Islets were dissociated in Accumax (Sigma-Aldrich, A7089) containing 10 units/mL DNase (Invitrogen, AM2222). After filtration (35-μm strainer) and centrifugation, cells were resuspended in Flow Cytometry Buffer (R&D Systems, FC001) containing 2 units/mL DNase, 0.5 mol/L EDTA, and 7-aminoactinomycin D (1:1,000; ThermoFisher, A1310). GFP^+/7-aminoactinomycin D^- cells were analyzed and isolated using an Aria II (BD Biosciences) and collected in Homogenization Solution (Promega, TM351; containing 1-thioglycerol).

RNA Purification and Quality Control

RNA was isolated from FACS-purified β-cells and whole islets using Maxwell 16 LEV simplyRNA Tissue Kit (Promega, TM351). RNA samples were analyzed using the Agilent 2100 Bioanalyzer. Only samples with an RNA integrity number >7 were used.

Library Assembly, Sequencing, and Analysis

RNA samples from FACS-purified β-cells were amplified using SMART-Seq v4 Ultra Low Input RNA Kit for Sequencing (Clontech, 634888; eight PCR cycles). cDNA libraries were constructed using the Low Input Library Prep Kit (Clontech, 634947). Paired-end sequencing of four replicates each of *Abcc8*$^{+/+}$*;MIP-GFP* and *Abcc8*$^{-/-}$*;MIP-GFP* samples was performed on an Illumina NextSeq 500 (75-nucleotide reads). Approximately 900 million raw reads were processed using TrimGalore 0.4.0. STAR (23) was used to align sequences to mm10 (Genome Reference Consortium Mouse Reference 38 [GRCm38]) and GENCODE comprehensive gene annotations (Release M8). HTSeq was used for counting reads mapped to genomic features (24), and DESeq2 was used for differential gene expression analysis (25).

Upstream Regulator Prediction

iRegulon (26) was used to predict gene regulatory networks. Default search parameters were used (20 kb centered on the

transcription start site, 7 species conservation). The enrichment score threshold was 3.0.

qRT-PCR

The High Capacity cDNA Reverse Transcription Kit (ThermoFisher, 4368814) was used to convert whole-islet RNA to cDNA. qRT-PCR was performed on an Applied Biosystems 7900HT using 2× SYBR Green PCR Master Mix (ThermoFisher, 4309155). Samples were analyzed in triplicate and normalized to *Hprt* expression. Primer sequences are listed in the Supplementary Data.

Statistical Analysis

Statistical significance was determined using the two-tailed Student *t* test. Data are represented as mean ± SEM. A threshold of $P < 0.05$ was used to declare significance.

RESULTS

Abcc8$^{-/-}$ β-Cells Exhibit Persistent Membrane Depolarization and Elevated $[Ca^{2+}]_i$

Previous studies have shown that single β-cells from mice lacking K_{ATP} channels, in contrast to normal mice, exhibit chronically elevated $[Ca^{2+}]_i$ and continuous action potential firing (16,27,28), whereas intact islets exhibit electrical bursting and Ca^{2+} oscillations (29,30). To definitively establish *Abcc8*$^{-/-}$ mice as a model for chronically elevated β-cell $[Ca^{2+}]_i$, we measured membrane potential at high (11 mmol/L) and low (2 mmol/L) glucose concentrations (Fig. 1*A* and *B*). *Abcc8*$^{-/-}$ β-cells exhibit action potentials in high glucose but fail to undergo membrane potential polarization in low glucose (Fig. 1*B*). Quantification of the changes in *Abcc8*$^{-/-}$ β-cell membrane potentials confirms that *Abcc8*$^{-/-}$ β-cells show no difference in membrane potential between high and low glucose, contrary to *Abcc8*$^{+/+}$ β-cells (Fig. 1*C* and *D*). However, *Abcc8*$^{-/-}$ β-cells exhibit a chronic elevation in $[Ca^{2+}]_i$, as shown by Ca^{2+}-imaging at both low and high glucose (Fig. 1*E*). Quantification of the area under the curve shows that *Abcc8*$^{-/-}$ β-cells have significantly higher $[Ca^{2+}]_i$ than *Abcc8*$^{+/+}$ β-cells at each time interval measured (Fig. 1*F*). In addition, by examining individual traces rather than averaged data and imaging over a longer period, we observe Ca^{2+} oscillations in *Abcc8*$^{-/-}$ islets under low glucose conditions, as previously reported (29,30), whereas *Abcc8*$^{+/+}$ islets exhibit consistently low Ca^{2+} levels (Supplementary Fig. 1). This indicates that although *Abcc8*$^{-/-}$ β-cells exhibit variable and oscillating $[Ca^{2+}]_i$ under euglycemic conditions, their mean $[Ca^{2+}]_i$ is elevated compared with *Abcc8*$^{+/+}$ β-cells.

Interestingly, despite having chronically elevated β-cell $[Ca^{2+}]_i$, *Abcc8*$^{-/-}$ mice have long been known to have surprisingly small disturbances in their plasma glucose concentrations (16). First, and as we previously reported (31), they exhibit outright hypoglycemia in the fasted state (Supplementary Fig. 3*A*). Second, they exhibit a trend toward mild hyperglycemia in the fed state (Supplementary Fig. 3*B*).

β-Cell Identity Becomes Compromised in *Abcc8*$^{-/-}$ Mice

During prolonged metabolic stress, β-cells can lose expression of functional markers and convert to other endocrine cell types (32). However, β-cell dedifferentiation has not been studied in the context of chronically elevated $[Ca^{2+}]_i$. Thus, we performed β-cell lineage tracing using *Abcc8*$^{-/-}$; *RIP-Cre*; *Rosa26*$^{LSL.YFP/+}$ mice. Although there was no evidence for β- to α-cell or β- to δ-cell *trans*-differentiation (Supplementary Fig. 2*A* and *B*), we observed an increase in yellow fluorescent protein (YFP)/PP coexpression (Fig. 2*C*). Most YFP/PP coexpressing cells are polyhormonal, expressing both PP and insulin (Fig. 2*A*), but a few cells (0.24% of all YFP-expressing cells and 10% of YFP/PP-coexpressing cells) (Supplementary Fig. 2*C*) no longer express insulin (Fig. 2*B*). Administration of a Ca^{2+}channel blocker to *Abcc8*$^{-/-}$ mice resulted in a lower number of insulin/PP-coexpressing cells, but the difference was not significant (Supplementary Fig. 2*D*). The loss of β-cell identity correlates with impaired glucose tolerance not attributable to β-cell death (Supplementary Fig. 3*A* and *C*). Complete dedifferentiation (e.g., YFP expression without hormone immunostaining), was only observed at a very low rate and was similar in both wild-type and knockout animals (0.19% and 0.21%, respectively) (Supplementary Fig. 2*E*).

RNA Expression Profiling

To determine how chronically elevated β-cell $[Ca^{2+}]_i$ affects gene expression, we performed RNA-Seq using FACS-purified β-cells from *Abcc8*$^{-/-}$;*MIP-GFP* mice at 8–9 weeks of age. Because the human growth hormone mini-gene within the *MIP-GFP* allele causes both human growth hormone expression and activation of STAT5 signaling (33), we used *MIP-GFP*–expressing mice as controls. Principal component and gene clustering analyses (Supplementary Fig. 4*B* and *C*), performed on RNA-Seq data from FACS-purified cells (Supplementary Fig. 4*A*), indicates that most of the top 500 differentially expressed genes cluster as expected. Differential expression analysis (Fig. 3*B* and Supplementary Table 1) revealed 4,208 differentially expressed genes (2,152 downregulated and 2,056 upregulated) in *Abcc8*$^{-/-}$ β-cells (adjusted $P < 0.05$). Approximately 90% are protein coding, 3% are noncoding RNAs, 2% are pseudogenes, and 3% are other types of processed transcripts (Fig. 3*A*).

Abcc8$^{-/-}$ β-Cells Exhibit Changes in Expression of Genes Involved in β-Cell Maturation, Ca^{2+} Signaling, Cell Adhesion, and Dedifferentiation

To correlate gene expression with the functional abnormalities of *Abcc8*$^{-/-}$ islets, we examined genes known to be highly enriched in mature β-cells and observed that *Ins1*, *Slc2a2*, *Neurod1*, *Gck*, *Glp1r*, *Npy*, several synaptotagmins, *Tph1*, *Tph2*, and *Egfr* are all downregulated (Fig. 3*C*). Conversely, *Ppy* is upregulated in *Abcc8*$^{-/-}$ β-cells, consistent with our observation of polyhormonal cells.

Because *Abcc8*$^{-/-}$ β-cells have a persistent increase in $[Ca^{2+}]_i$, we examined genes with well-defined roles in Ca^{2+}

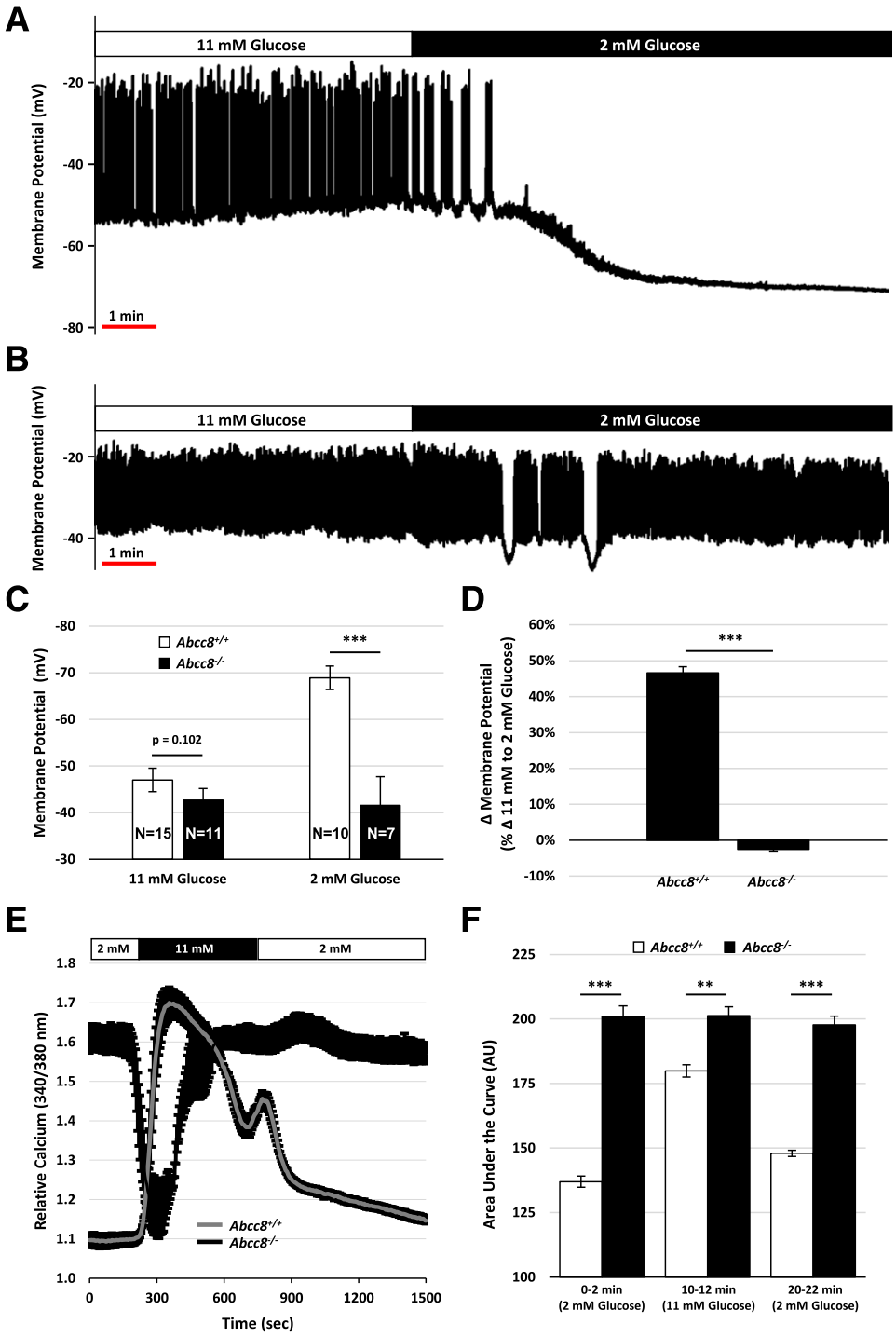

Figure 1—*Abcc8*$^{-/-}$ β-cells exhibit persistent membrane depolarization and elevated $[Ca^{2+}]_i$. A perforated patch recording technique was used to monitor the membrane potential of *Abcc8*$^{+/+}$ and *Abcc8*$^{-/-}$ β-cells in whole islets. *A*: *Abcc8*$^{+/+}$ β-cells display normal activity at 11 mmol/L glucose and become hyperpolarized in response to 2 mmol/L glucose (representative recording). *B*: *Abcc8*$^{-/-}$ β-cells display activity similar to *Abcc8*$^{+/+}$ β-cells at 11 mmol/L glucose (with a trend toward a depolarized plateau potential); however, their activity remains statistically unchanged in response to 2 mmol/L glucose (representative recording). *C*: Quantification of the potentials of *Abcc8*$^{+/+}$ and *Abcc8*$^{-/-}$ β-cells at 11 mmol/L and 2 mmol/L glucose. *Abcc8*$^{+/+}$ β-cells become significantly more polarized in response to 2 mmol/L glucose, but there is no difference between *Abcc8*$^{-/-}$ β-cells at 11 mmol/L and 2 mmol/L glucose. *D*: Quantification of the percentage change in membrane potential between 11 mmol/L and 2 mmol/L glucose for *Abcc8*$^{+/+}$ and *Abcc8*$^{-/-}$ β-cells. The membrane potential of *Abcc8*$^{+/+}$ β-cells changes significantly more than *Abcc8*$^{-/-}$ β-cells. *E*: $[Ca^{2+}]_i$ was monitored in *Abcc8*$^{+/+}$ and *Abcc8*$^{-/-}$ islets with Fura-2 acetoxymethyl ester. Islets were equilibrated in 2 mmol/L glucose, stimulated with 11 mmol/L glucose, and returned to 2 mmol/L glucose, as indicated by the bars above the traces (overall averages are shown). *F*: Area under the curve of $[Ca^{2+}]_i$ was quantified at intervals representing low glucose conditions (0–2 min), glucose-stimulation (10–12 min), and a return to low glucose (20–22 min). Data are an average of $n \geq 21$ islets from 3 animals. $^{**}P < 0.01$; $^{***}P < 0.001$.

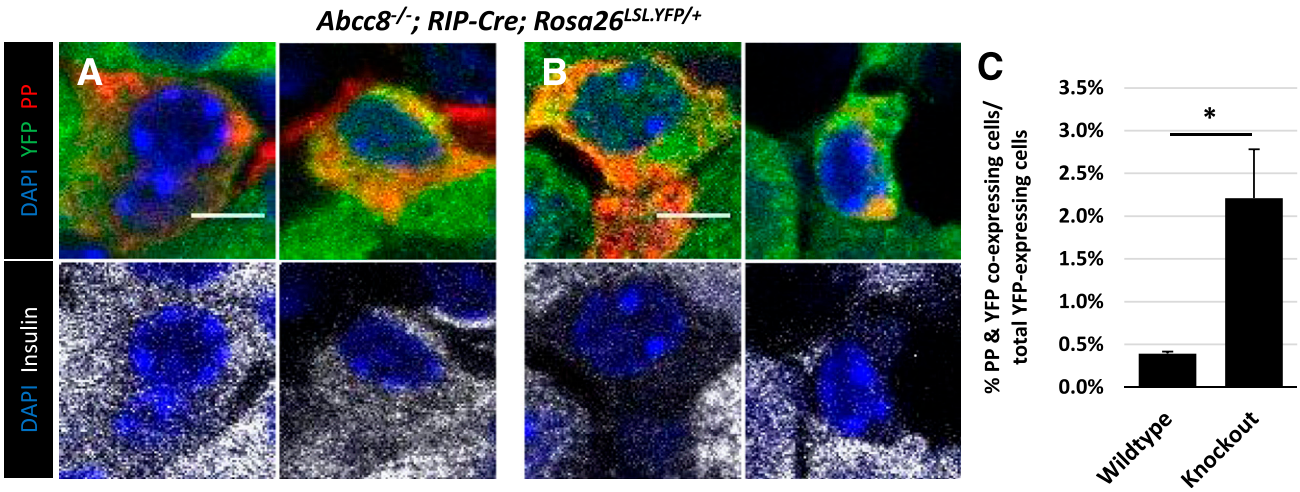

Figure 2—Loss of strict β-cell identity in *Abcc8*$^{-/-}$ mice. We performed β-cell lineage tracing using *Abcc8*$^{-/-}$*;RIP-Cre;R26*$^{LSL.YFP/+}$ animals and assessed β-cell dedifferentiation at 12 weeks of age. *A*: Representative examples of polyhormonal cells coexpressing YFP, PP, and insulin. *B*: Representative examples of YFP-labeled cells that are expressing PP but not expressing insulin. *C*: Quantification of PP/YFP double$^+$ cells shows an increase in their occurrence in *Abcc8*$^{-/-}$*;RIP-Cre; R26*$^{LSL.YFP/+}$ mice compared with *Abcc8*$^{+/+}$*;RIP-Cre; R26*$^{LSL.YFP/+}$ mice at 12 weeks of age. n = 3–4 animals, 10–15 islets counted per animal. Scale bars = 5 μm. *$P < 0.05$.

binding or signaling, such as *Myo7a*, a Ca^{2+}/calmodulin-binding myosin motor protein, *Pcp4*, a calmodulin binding protein known to protect neurons from Ca^{2+}-induced toxicity (34), and *Cacng3*, a subunit of a voltage-dependent Ca^{2+} channel, and found their expression was elevated. Similarly, we observed that *Nfatc1*, *Mef2c*, and *Mef2d,* three calcium-regulated transcription factors; *Camk1d*, *Camkk1*, and *Camkk2,* three kinases involved in calcium-signaling; and *S100a1*, *S100a3*, *S100a4*, *S100a6*, and *S100a13*, five EF-hand Ca^{2+} binding proteins, were also upregulated (Fig. 3*C*).

Quantitation of islet cell types in *Abcc8*$^{-/-}$ mice revealed fewer β-cells, more α-, δ-, and PP cells, and a progressive redistribution of non–β-endocrine cells to the islet core (Supplementary Fig. 5). To correlate gene expression with this disrupted islet architecture, we examined expression of cell adhesion molecules, hypothesizing that a reduction in such genes could result in loss of islet structure. Consistently, we observed a reduction in multiple cell adhesion molecules, including *Cldn1, Cldn3, Cldn8, Cldn23*, and *Ocln*, genes involved in tight junctions; *Cdh1, Cdh7, Cdh8, Cdh13,* and *Cdh18*, encoding cadherins; *Cdhr1*, a cadherin-related protein; *Pcdhb15* and *Pcdhb22*, encoding protocadherins; and *Vcam1*, a vascular cell adhesion molecule (Fig. 3*C*).

Aldh1a3, a retinaldehyde dehydrogenase recently suggested to be a marker for β-cell dedifferentiation (35), is 27-fold upregulated in *Abcc8*$^{-/-}$ β-cells by RNA-Seq (Fig. 3*C*). In addition, six other genes (*Serpina7*, *Aass*, *Asb11*, *Penk*, *Fabp3*, and *Tcea1*) enriched in dedifferentiated β-cells (35) are upregulated in *Abcc8*$^{-/-}$ β-cells (Fig. 3*C*). Coimmunostaining with insulin indicates that although ALDH1A3 is expressed in only 0.4% of *Abcc8*$^{+/+}$ β-cells, it is present in 29.1% of *Abcc8*$^{-/-}$ β-cells (Fig. 4*A* and *B*). However, this fraction was reduced to 11.4% in *Abcc8*$^{-/-}$ mice administered the Ca^{2+} channel blocker verapamil (Fig. 4*A* and *B*), further suggesting that a chronic increase in $[Ca^{2+}]_i$ impairs the maintenance of cell identity.

S100a6 and *S100a4* Are Markers of Excitotoxicity in β-Cells

To identify genes that could serve as markers of β-cell excitotoxicity, we analyzed *S100a6* and *S100a4*. Both genes are appealing targets because of their functions as EF-hand Ca^{2+} binding proteins, the association of *S100a6* with insulin secretion (36), and the increased expression of members of the *S100* gene family in islets from humans with hyperglycemia (37). Moreover, they are among the most highly upregulated genes in *Abcc8*$^{-/-}$ β-cells, with *S100a6* and *S100a4* increasing 37- and 5-fold, respectively. S100A6 is only expressed in 2.8% of *Abcc8*$^{+/+}$ β-cells but is expressed in 38.4% of *Abcc8*$^{-/-}$ β-cells (Fig. 4*C* and *D*). In addition, qRT-PCR using whole-islet RNA confirms the upregulation of *S100a6* and *S1004* in *Abcc8*$^{-/-}$ islets (Fig. 5*A*).

To determine whether the observed changes in *S100a6* and *S100a4* expression in *Abcc8*$^{-/-}$ β-cells are the result of chronically elevated $[Ca^{2+}]_i$ and not some other mechanism, we treated wild-type islets with KCl or tolbutamide and found that membrane depolarization is associated with an increase in both *S100a6* and *S100a4* expression (Fig. 5*B–E*), mirroring the expression pattern in *Abcc8*$^{-/-}$ β-cells. These changes were reversed when islets were treated with both a depolarizing agent and the Ca^{2+}channel inhibitor verapamil (Fig. 5*B–E*). Moreover, the expression of *S100a6* and *S100a4* was decreased when Ca^{2+} influx is pharmacologically inhibited in *Abcc8*$^{-/-}$ mice (Fig. 5*F* and *G*). These results suggest that *S100a6* and *S100a4* expression in *Abcc8*$^{-/-}$ β-cells is tightly correlated with $[Ca^{2+}]_i$. Finally, coimmunostaining with S100A6 and ALDH1A3 revealed that 15.4 ± 2.1% of insulin-expressing cells in *Abcc8*$^{-/-}$ mice express both S100A6 and ALDH1A3 (Fig. 4*E*).

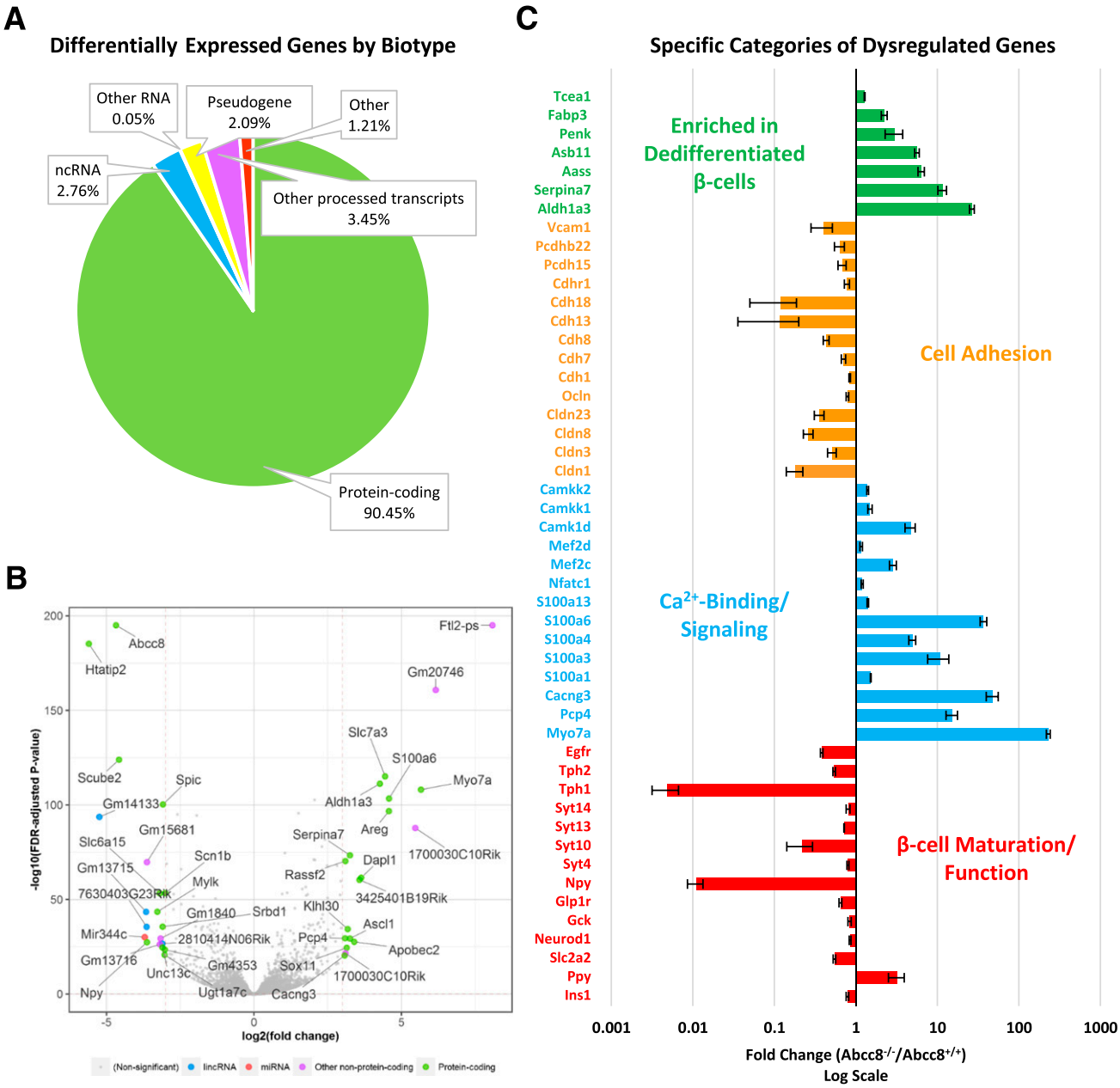

Figure 3—RNA-sequencing of *Abcc8*$^{-/-}$ β-cells. We performed RNA-sequencing of FACS-purified β-cells from *Abcc8*$^{-/-}$*;MIP-GFP* and *Abcc8*$^{+/+}$*;MIP-GFP* animals at 8–9 weeks of age. *A*: Pie chart shows the percentage of differentially regulated genes that fall into biotype categories of protein-coding, noncoding RNA (ncRNA), other RNA, pseudogene, other processed transcripts, and other types of transcripts. *B*: Volcano plot shows the most differentially expressed genes in *Abcc8*$^{-/-}$*;MIP-GFP* β-cells based on the $-\log_{10}$ (false discovery rate [FDR]–adjusted *P* value) and the $\log_2$ (fold change). Genes with a $\log_2$ (fold change) greater than three are labeled and grouped into categories by biotype characterization. *C*: Selected differentially expressed genes in *Abcc8*$^{-/-}$*;MIP-GFP* β-cells. *Abcc8*$^{-/-}$*;MIP-GFP* β-cells exhibit a decrease in expression of genes associated with β-cell maturation/function, an increase in expression of genes associated with Ca^{2+}signaling, Ca^{2+}binding, or Ca^{2+}-dependent gene expression, a decrease in expression of genes associated with cell adhesion, and an increase in genes that are enriched in a population of dedifferentiated β-cells, as indicated by the fold change in selected genes from our RNA-Seq data set. All genes shown were manually selected and have FDR-adjusted *P* values <0.05.

Prediction of Upstream Regulators

To determine whether differentially expressed genes in *Abcc8*$^{-/-}$ β-cells might share common upstream regulators, we used iRegulon, a program that identifies common DNA binding motifs in coexpressed genes (26). Analysis of the top 500 upregulated genes revealed binding sites for ASCL1, CEBPG, and RARG in many genes, with some genes, including *Aldh1a3*, containing binding sites for all three of these transcriptional regulators (Fig. 6*A*, Supplementary Table 2, and Supplementary Fig. 6). Interestingly, all three of these predicted regulators are upregulated in *Abcc8*$^{-/-}$ β-cells (Fig. 6*C*). Conversely, analysis of the top 500 downregulated

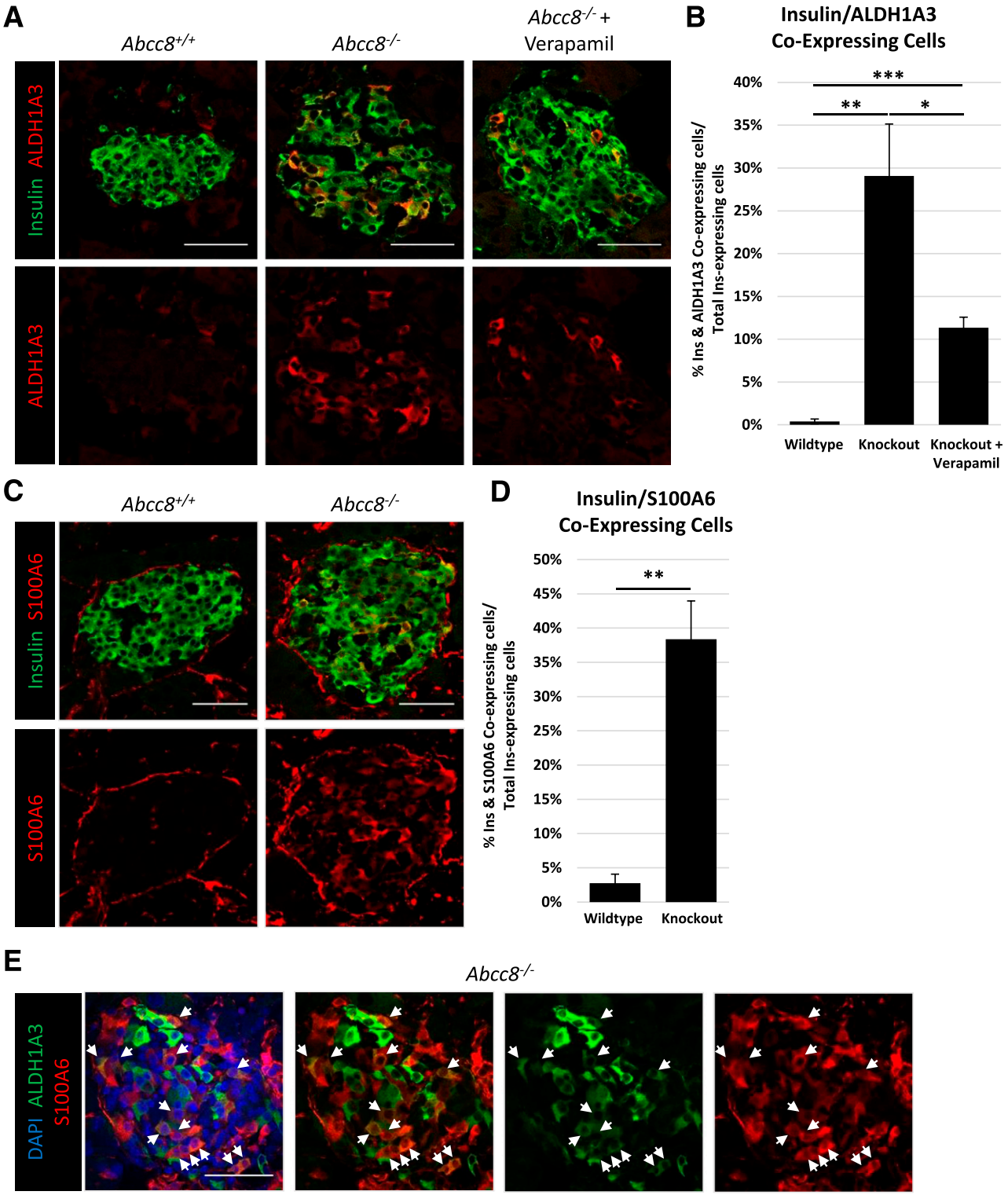

Figure 4—Heterogeneous expression of S100A6 and ALDH1A3. *A*: Coimmunostaining of ALDH1A3, a potent marker of dedifferentiated β-cells, and insulin in pancreatic sections from *Abcc8*$^{+/+}$, *Abcc8*$^{-/-}$, and *Abcc8*$^{-/-}$ mice given verapamil. *B*: Quantification of *A* showing the percentage of insulin (Ins) and ALDH1A3 coexpressing cells in each group. Verapamil treatment partially rescues the percentage of ALDH1A3-expressing β-cells in *Abcc8*$^{-/-}$ mice. *C*: Coimmunostaining of S100A6 and insulin in *Abcc8*$^{+/+}$ and *Abcc8*$^{-/-}$ pancreatic sections. *D*: Quantification of *C* showing the percentage of insulin-expressing cells that coexpress S100A6 in *Abcc8*$^{+/+}$ and *Abcc8*$^{-/-}$ mice. *E*: Coimmunostaining of ALDH1A3 and S100A6 shows that there is not strict colocalization of these two factors, again emphasizing the heterogeneous nature of β-cell failure. The arrows indicate cells that coexpress ALDH1A3 and S100A6. $n = 3$ animals, 8–12 islets counted per animal. Scale bars = 50 μm. *$P < 0.05$; **$P < 0.01$; ***$P < 0.001$.

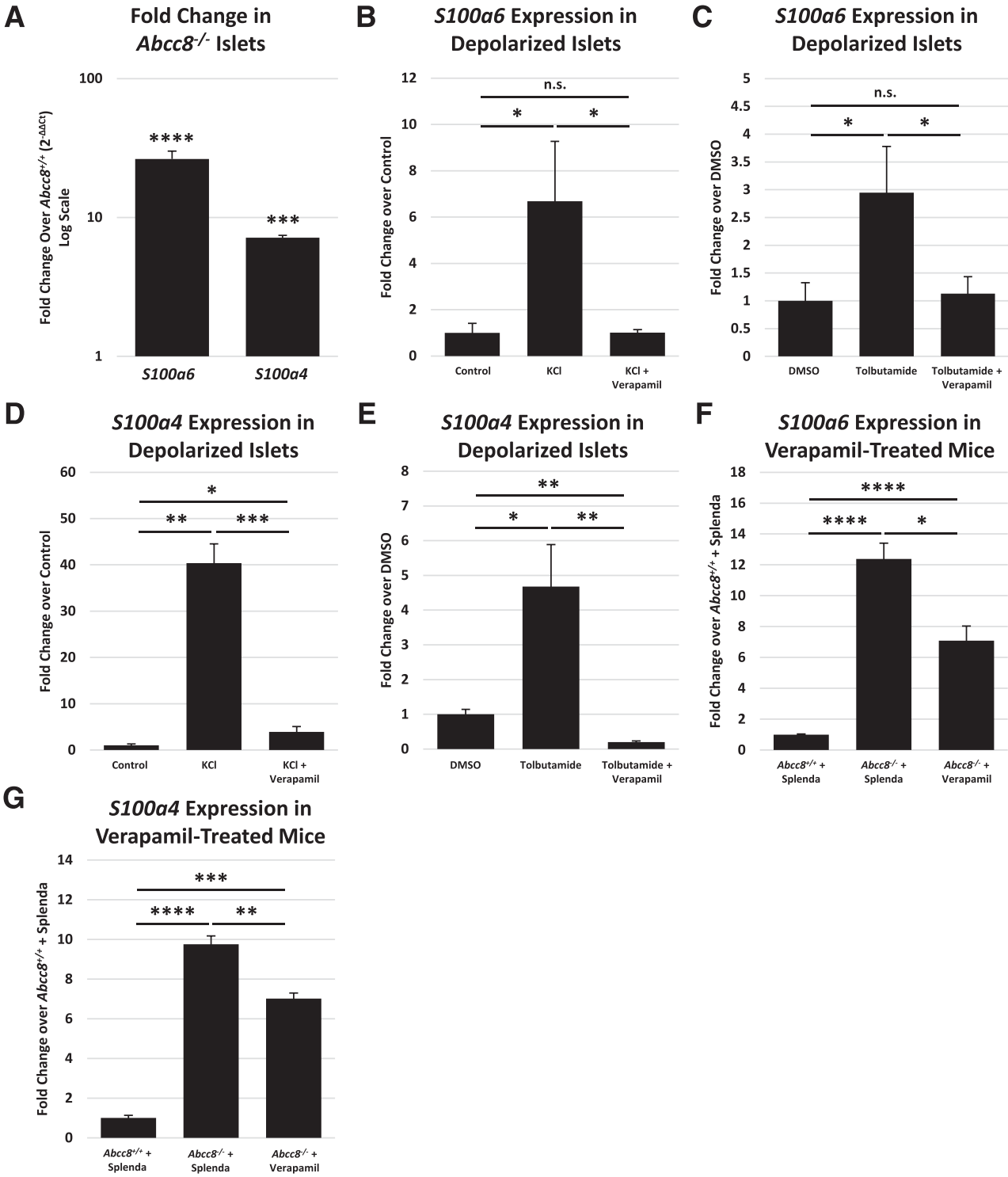

Figure 5—*S100a6* and *S100a4* serve as markers of excitotoxicity in β-cells. *A*: qRT-PCR using whole-islet RNA confirms upregulation of *S100a6* and *S100a4* in *Abcc8*$^{-/-}$ islets compared with *Abcc8*$^{+/+}$ islets. *B–E*: qRT-PCR using whole-islet RNA from wild-type islets treated with 100 μmol/L tolbutamide or 20 mmol/L KCl, with or without 50 μmol/L verapamil, for 24 h. *S100a6* (*B* and *C*) and *S100a4* (*D* and *E*) are significantly upregulated in response to membrane depolarization, but this effect is negated when Ca^{2+} influx is blocked. *F* and *G*: qRT-PCR using whole-islet RNA from animals administered verapamil (1 mg/mL) in the drinking water for 3 weeks indicates that expression of both *S100a6* and *S100a4* is significantly downregulated when Ca^{2+} influx is inhibited. n.s. = not significant. *$P < 0.05$; **$P < 0.01$; ***$P < 0.001$; ****$P < 0.0001$.

genes predicts binding sites for TEAD1, HNF1A, and ZFP647 (Fig. 6*B*, Supplementary Table 3, and Supplementary Fig. 7). However, the expression of these regulators is unchanged in *Abcc8*$^{-/-}$ β-cells (Fig. 6*C*).

Ascl1 Is Regulated by $[Ca^{2+}]_i$ in β-Cells

Because *Ascl1* is 22-fold upregulated in *Abcc8*$^{-/-}$;*MIP-GFP* β-cells (Fig. 3*B*) and 24-fold upregulated in *Abcc8*$^{-/-}$ islets (Fig. 6*D*) and has been shown by chromatin immunoprecipitation (ChIP) sequencing or ChIP PCR to bind near 51% of the predicted targets (38–40), we studied its responsiveness to changes in $[Ca^{2+}]_i$ in isolated islets. Consistent with *Ascl1* being regulated by $[Ca^{2+}]_i$, its expression increases in response to membrane depolarization, an effect that is reversed when Ca^{2+} influx is inhibited by verapamil, both in isolated islets (Fig. 6*E*) and in mice (Fig. 6*F*). These results support the idea that ASCL1 could play a central role in regulating gene expression in β-cells with chronically elevated $[Ca^{2+}]_i$.

DISCUSSION

Abcc8$^{-/-}$ β-Cells Exhibit Elevated Basal $[Ca^{2+}]_i$

Abcc8$^{-/-}$ β-cells have been previously shown to have altered $[Ca^{2+}]_i$ homeostasis, as would be expected in the absence of K_{ATP} channels (16,27–30). We similarly observed that *Abcc8*$^{-/-}$ β-cells exhibit both persistent depolarization and an elevated mean $[Ca^{2+}]_i$ compared with *Abcc8*$^{+/+}$ islets (Fig. 1). Interestingly, although *Abcc8*$^{-/-}$ β-cells exhibit Ca^{2+} oscillations in substimulatory glucose (Supplementary Fig. 1), as has been previously reported (29,30), we did not

A

Regulator	Enrichment Score	No. Predicted Targets
ASCL1	3.704	271
CEBPG	3.143	199
RARG	3.062	155

B

Regulator	Enrichment Score	No. Predicted Targets
TEAD1	3.848	52
HNF1A	3.313	70
ZFP647	3.277	163

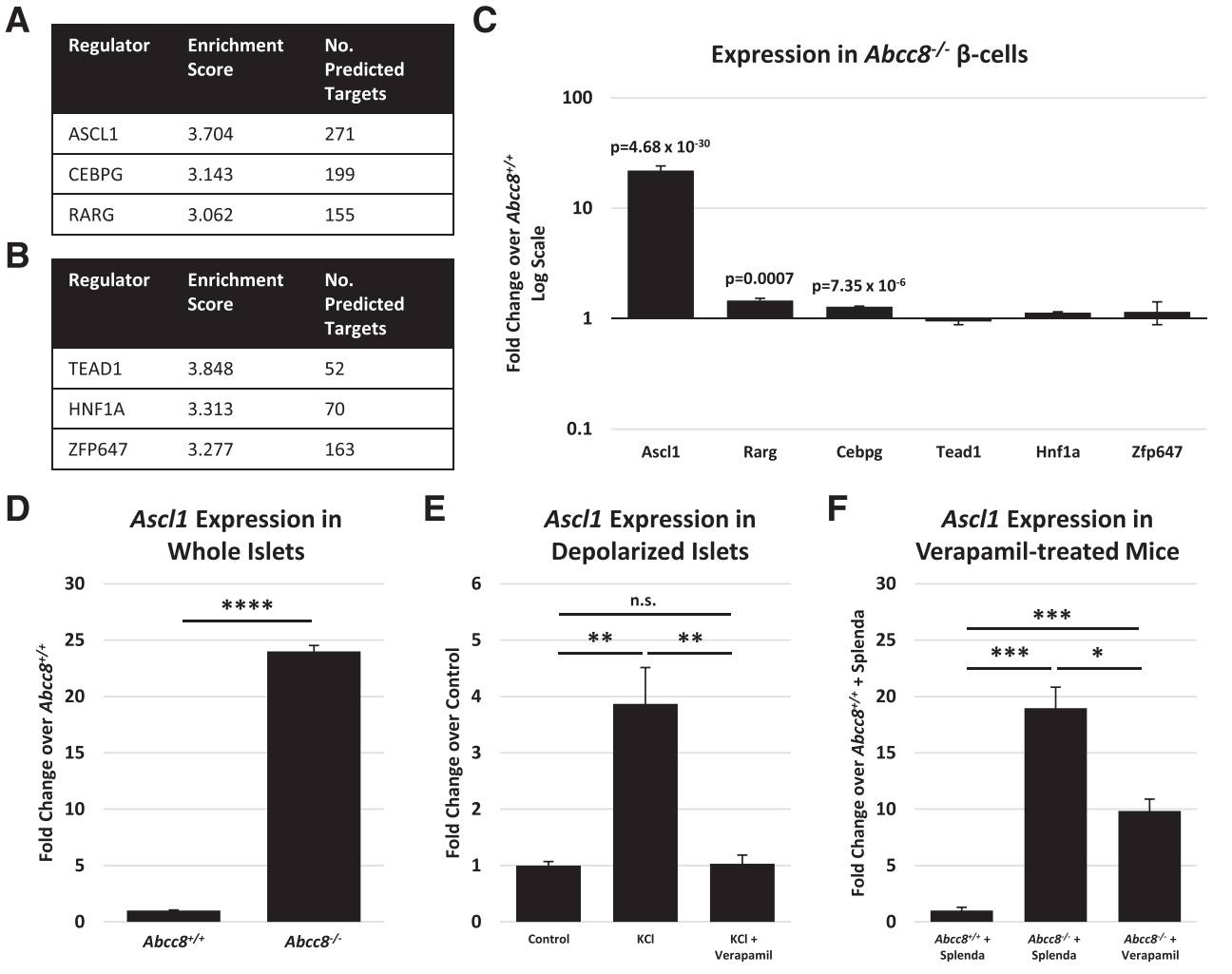

Figure 6—Upstream regulator prediction using iRegulon. Using the top 500 up- and downregulated genes in *Abcc8*$^{-/-}$ β-cells, we used iRegulon to predict common upstream regulators based on enriched DNA-binding motifs. Tables summarize the top three predicted regulators of upregulated (*A*) and downregulated (*B*) genes, their enrichment scores, and the number of predicted targets. *C*: Expression of the predicted regulators in *Abcc8*$^{-/-}$ β-cells, as determined by RNA-Seq. *D*: qRT-PCR using whole-islet RNA confirms upregulation of *Ascl1* in *Abcc8*$^{-/-}$ islets compared with *Abcc8*$^{+/+}$ islets. *E*: qRT-PCR for *Ascl1* using whole-islet RNA from wild-type islets treated with 20 mmol/L KCl, with or without 50 μmol/L verapamil, for 24 h. *F*: qRT-PCR using whole-islet RNA from animals administered verapamil. n.s. = not significant. **P* < 0.05; ***P* < 0.01; ****P* < 0.001; *****P* < 0.0001.

consistently observe oscillations in membrane potential, as has been observed in β-cells lacking K_{ATP} channels. This may be the result of the short duration of the recordings or to our use of the patch-clamp technique rather than intracellular microelectrodes, which limits the detection of oscillations in membrane potential (29). Regardless, *Abcc8*$^{-/-}$ β-cells experience more persistent membrane depolarization and elevated mean $[Ca^{2+}]_i$ compared with wild-type β-cells, and the downstream effects on gene expression are likely to be the same. We also observed a transient drop in $[Ca^{2+}]_i$ in *Abcc8*$^{-/-}$ islets after glucose stimulation (Fig. 1*E*) that was not seen in *Abcc8*$^{+/+}$ islets. This drop is the result of brief membrane hyperpolarization caused by transient activation of the sodium potassium ATPase (29) and has been observed previously in islets treated with K_{ATP} channel inhibitors (41) as well as in other K_{ATP} channel–deficient mice (29).

Abcc8$^{-/-}$ β-Cells Exhibit Dysregulated Gene Expression

By performing RNA-Seq on purified pancreatic β-cell populations from both *Abcc8*$^{-/-}$ and *Abcc8*$^{+/+}$ mice, we found that the expression of 4,208 genes was perturbed. Some of these genes, including *S100a6, Myo7a, Pcp4, Cacng3, Mef2c,* and *Camk1d,* are known to be involved in calcium binding and signaling (Fig. 3*C*). The *S100* gene family, for instance, modulates the activity of other proteins on calcium binding (42). Moreover, S100A6 specifically promotes Ca^{2+}-stimulated insulin release (36). *Camk1d*, *Camkk1*, and *Camkk2*, three protein kinases, *Myo7a*, a myosin motor protein, and *Mef2d* and *Mef2c,* are involved in Ca^{2+}/calmodulin-dependent signaling or are regulated by $[Ca^{2+}]_i$ (43,44). However, the alteration of some Ca^{2+}-regulated genes does not imply that all of the gene expression changes we observed are caused by changes in $[Ca^{2+}]_i$. Although we have demonstrated that changes in *S100a6*, *S100a4,* and *Ascl1* expression are tightly linked to membrane potential (Figs. 5*B* and *E* and 6*E*), a similar analysis has not been performed for the remaining genes. Thus, although it is likely that a substantial fraction of the dysregulated genes are the result of altered $[Ca^{2+}]_i$ homeostasis, other mechanisms, such as paracrine and/or neuronal signaling, may also be involved. Additional studies are necessary to determine which changes are directly attributable to chronically elevated $[Ca^{2+}]_i$ and which are the result of other signaling mechanisms and/or compensatory adaptations.

Compromised β-Cell Identity in *Abcc8*$^{-/-}$ Mice

Recent studies have suggested that β-cell dedifferentiation contributes to the development of T2D (32,35). Among the genes affected in *Abcc8*$^{-/-}$ β-cells are many known to be involved in maintaining β-cell identity and/or function, such as *Ins1*, *Slc2a2*, *Neurod1*, *Gck,* and *Syt10* (Fig. 3*C*). However, some of the transcription factors previously associated with β-cell dedifferentiation (32), including *Mafa*, *Pdx1*, *Nkx6.1*, *FoxO1*, *Ngn3*, *Oct4*, and *Nanog*, are unchanged. This difference may explain the modest loss of β-cell identity observed in *Abcc8*$^{-/-}$ mice, with only 2.21% of β-cells undergoing *trans*-differentiation to insulin/PP polyhormonal or PP monohormonal cells (Fig. 2*C*). Although treatment with a Ca^{2+} channel blocker did not statistically reverse the insulin/PP polyhormonal cells, its use resulted in a decrease in the percentage of *Abcc8*$^{-/-}$ β-cells expressing the dedifferentiation marker ALDH1A3 (Fig. 4*B*), further suggesting that a chronic increase in $[Ca^{2+}]_i$ may contribute to loss of β-cell identity. In this regard, it is important to distinguish our results, which reflect the loss of K_{ATP} channels, from studies using K_{ATP} channel gain-of-function mutants (45,46). The current study examines the effects of elevated $[Ca^{2+}]_i$ in a nearly euglycemic setting, whereas the latter reflects decreased $[Ca^{2+}]_i$ in a hyperglycemic setting.

Two Potential Genetic Markers for Elevated $[Ca^{2+}]_i$

Our studies identified two genes, *S100a6* and *S100a4*, that were highly upregulated in *Abcc8*$^{-/-}$ β-cells and were also acutely regulated by treatment with depolarizing agents and a Ca^{2+}channel blocker in isolated islets (Fig. 5*B* and *E*). The administration of a Ca^{2+} channel blocker to *Abcc8*$^{-/-}$ mice only partially rescued the expression of *S100a6* or *S100a4* (Fig. 5*F* and *G*), but this may be the result of inadequate dosing or a treatment duration that was too short to overcome the effects of the *Abcc8* gene knockout. However, it is also possible that these genes are only partially regulated by Ca^{2+} influx in vivo. Regardless, our data strongly suggest that *S100a6* and *S100a4* are regulated by Ca^{2+} in the β-cell and that they may serve as markers for β-cell excitotoxicity. In support of this, members of the S100 gene family, including *S100A3, S100A6, S100A10, S100A11,* and *S100A16,* have been associated with hyperglycemia in human islets (37), and *S100A6* was specifically shown to be positively correlated with BMI in β-cells from donors with T2D (47). Neither gene was altered in two recent single-cell sequencing studies of people with T2D (47,48), but the sequencing depth was very shallow.

Effects of a Sustained Increase in $[Ca^{2+}]_i$ on Islet Morphology

Perturbations in Ca^{2+} signaling also provide a compelling explanation for the disrupted islet morphology observed in K_{ATP}-channel knockout mice (Supplementary Fig. 5). $[Ca^{2+}]_i$ is required for maintenance of tight junctions and adherens junctions, and focal adhesion disassembly occurs in response to elevated $[Ca^{2+}]_i$ (49). Accordingly, among the downregulated genes are many that encode cell adhesion molecules, such as *Ocln, Tln1*, and *Cdh1* (Fig. 3*C*), suggesting that a Ca^{2+}-dependent gradual breakdown of cell-to-cell contacts may be responsible for the altered islet morphology.

Identification of Putative Upstream Regulators

Bioinformatics analysis of genes whose expression was increased in the *Abcc8*$^{-/-}$ mice identified ASCL1, CEBPG, and RARG as possible upstream regulators (Fig. 6*A*). ASCL1, also known as MASH1, is important for neuronal commitment and differentiation (50). Retinoic acid receptors,

including RARG, play a role in both endocrine cell development and maintenance of proper insulin secretion and β-cell mass (51). Finally, CEBPB, a closely related protein to CEBPG, represses the insulin promoter under conditions of chronically elevated glucose, and its accumulation in β-cells increases vulnerability to endoplasmic reticulum stress (52,53). Although our computational analysis is purely predictive, it is partially validated by the fact that 51% of the ASCL1 target genes and 60% of the RARG binding sites were established by ChIP-Seq or ChIP-PCR (38–40,54). Importantly, *S100a4* is among the ASCL1 targets that have been experimentally validated (38–40), and our in-depth analysis of *Ascl1* strongly supports its regulation by $[Ca^{2+}]_i$, consistent with our model. Conversely, analysis of genes that are downregulated by $[Ca^{2+}]_i$ predicts binding sites for TEAD1, HNF1A, and ZFP647 (Fig. 6*B*). Although *Tead1* gene expression is unaffected in *Abcc8*$^{-/-}$ β-cells, the activity of TEAD1, a member of the Hippo pathway that interacts with YAP/TAZ to promote proliferation, is directly inhibited by Ca^{2+} (55). Furthermore, because a gene knockout of *Hnf1a* results in β-cell failure and diabetes (56), a predicted decrease in its activity could explain the decrease in genes involved in β-cell function in *Abcc8*$^{-/-}$ β-cells.

Does Excitotoxicity Contribute to β-Cell Failure?

Our studies, together with findings of others (15,16,27–30), indicate that the absence of functional K_{ATP} channels in *Abcc8*$^{-/-}$ mice causes a chronic elevation of β-cell $[Ca^{2+}]_i$, an impairment of β-cell identity, alterations in islet cell numbers and morphology, and very significant perturbations in β-cell gene expression. Although the elevation of $[Ca^{2+}]_i$ in *Abcc8*$^{-/-}$ β-cells, caused by the total absence of K_{ATP}-channels, is persistent and severe, a less severe or persistent elevation in mean $[Ca^{2+}]_i$ may also occur in patients with prediabetes or T2D, when hyperglycemia chronically stimulates insulin secretion, or when a sulfonylurea is given as therapy for T2D. Interestingly, although *Abcc8*$^{-/-}$ mice exhibit impaired glucose tolerance at 12 weeks of age, they do not go on to develop T2D, at least in the time frame studied here. This suggests that the impairments in β-cell identity and islet morphology are insufficient themselves to cause β-cell failure. However, β-cell excitotoxicity, acting in combination with other metabolic stresses, may accelerate the loss of functional β-cells, perhaps by dedifferentiation or glucolipotoxicity. Regardless, our findings provide new insights into transcriptional responses that occur within β-cells when they are subjected to chronically elevated $[Ca^{2+}]_i$ and suggest a model (Fig. 7) that involves the coordinated interactions of a network of Ca^{2+}-responsive genes and upstream transcriptional modulators. This network may exist to balance both the positive and negative effects that $[Ca^{2+}]_i$ is known to have on β-cell function and mass.

RNA-Seq data are available in ArrayExpress (www.ebi.ac.uk/arrayexpress) under accession number E-MTAB-4726.

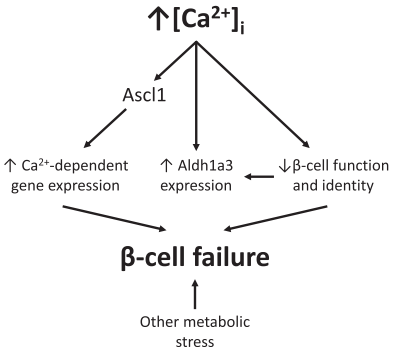

Figure 7—Model shows the effects of chronically elevated $[Ca^{2+}]_i$ in the β-cell. Our results suggest that there is a putative gene regulatory network mediating the effects of chronically elevated $[Ca^{2+}]_i$ in the β-cell. First, the effects of elevated $[Ca^{2+}]_i$ may be at least partly mediated through the predicted regulator *Ascl1*, causing an elevation in Ca^{2+}-dependent gene expression changes. Second, an elevated $[Ca^{2+}]_i$ may also contribute to the loss of β-cell function and stable β-cell identity, as evidenced by elevation in *Aldh1a3* expression as well as the presence of polyhormonal cells. These effects mediated by chronically elevated $[Ca^{2+}]_i$ combined with other metabolic stresses may contribute to β-cell failure in T2D.

Acknowledgments. The authors thank the Vanderbilt Islet Procurement and Analysis Core for performing multiple islet isolations, Vanderbilt Technologies for Advanced Genomics (VANTAGE) for performing cell sorting and RNA-Seq, the Vanderbilt Cell Imaging Shared Resource for helping to acquire images, the Vanderbilt Tissue Pathology Shared Resource for processing and sectioning paraffin-embedded tissues, and the Vanderbilt Transgenic Mouse/ESC Shared Resource for reconstituting mice with the *Abcc8* null allele. The authors also thank Guoqiang Gu and Roland Stein of Vanderbilt University for reading the manuscript and Jody Peters, Katherine Boyer, and Lauren Stiehle, also of Vanderbilt University, for technical assistance.

Funding. These studies were partly supported by National Institutes of Health/National Institute of Diabetes and Digestive and Kidney Diseases grants DK-72473 and DK-89523 to M.A.M. and DK-020593 to Vanderbilt Islet Procurement and Analysis Core, Vanderbilt Cell Imaging Shared Resource, and Vanderbilt Transgenic Mouse/ESC Shared Resource and by National Cancer Institute grant CA-68485 to Vanderbilt Cell Imaging Shared Resource and Vanderbilt Transgenic Mouse/ESC Shared Resource.

Duality of Interest. No potential conflicts of interest relevant to this article were reported.

Author Contributions. J.S.S. and M.A.M. designed the study and wrote the manuscript. J.S.S., H.W.C., and J.T.O. performed experiments and analyzed data. J.-P.C. performed RNA-Seq data processing, alignment, and differential gene expression analysis and edited the manuscript. M.T.D., P.K.D., and D.A.J. performed membrane potential measurements and calcium imaging and analyzed the data. A.B.O. contributed to study design and edited the manuscript. M.A.M. supervised and funded the experiments. M.A.M. is the guarantor of this work and, as such, had full access to all the data in the study and takes responsibility for the integrity of the data and the accuracy of the data analysis.

References

1. Muoio DM, Newgard CB. Mechanisms of disease: molecular and metabolic mechanisms of insulin resistance and beta-cell failure in type 2 diabetes. Nat Rev Mol Cell Biol 2008;9:193–205

2. Poitout V, Robertson RP. Glucolipotoxicity: fuel excess and beta-cell dysfunction. Endocr Rev 2008;29:351–366

3. Tornovsky-Babeay S, Dadon D, Ziv O, et al. Type 2 diabetes and congenital hyperinsulinism cause DNA double-strand breaks and p53 activity in β cells. Cell Metab 2014;19:109–121
4. Arundine M, Tymianski M. Molecular mechanisms of calcium-dependent neurodegeneration in excitotoxicity. Cell Calcium 2003;34:325–337
5. Heit JJ, Apelqvist AA, Gu X, et al. Calcineurin/NFAT signalling regulates pancreatic beta-cell growth and function. Nature 2006;443:345–349
6. Soleimanpour SA, Crutchlow MF, Ferrari AM, et al. Calcineurin signaling regulates human islet beta-cell survival. J Biol Chem 2010;285:40050–40059
7. Dadi PK, Vierra NC, Ustione A, Piston DW, Colbran RJ, Jacobson DA. Inhibition of pancreatic β-cell Ca2+/calmodulin-dependent protein kinase II reduces glucose-stimulated calcium influx and insulin secretion, impairing glucose tolerance. J Biol Chem 2014;289:12435–12445
8. Screaton RA, Conkright MD, Katoh Y, et al. The CREB coactivator TORC2 functions as a calcium- and cAMP-sensitive coincidence detector. Cell 2004;119:61–74
9. Blanchet E, Van de Velde S, Matsumura S, et al. Feedback inhibition of CREB signaling promotes beta cell dysfunction in insulin resistance. Cell Reports 2015;10:1149–1157
10. Epstein PN, Overbeek PA, Means AR. Calmodulin-induced early-onset diabetes in transgenic mice. Cell 1989;58:1067–1073
11. Bernal-Mizrachi E, Cras-Méneur C, Ye BR, Johnson JD, Permutt MA. Transgenic overexpression of active calcineurin in beta-cells results in decreased beta-cell mass and hyperglycemia. PLoS One 2010;5:e11969
12. Porat S, Weinberg-Corem N, Tornovsky-Babaey S, et al. Control of pancreatic β cell regeneration by glucose metabolism. Cell Metab 2011;13:440–449
13. Xu G, Chen J, Jing G, Shalev A. Preventing β-cell loss and diabetes with calcium channel blockers. Diabetes 2012;61:848–856
14. Shiota C, Rocheleau JV, Shiota M, Piston DW, Magnuson MA. Impaired glucagon secretory responses in mice lacking the type 1 sulfonylurea receptor. Am J Physiol Endocrinol Metab 2005;289:E570–E577
15. Winarto A, Miki T, Seino S, Iwanaga T. Morphological changes in pancreatic islets of KATP channel-deficient mice: the involvement of KATP channels in the survival of insulin cells and the maintenance of islet architecture. Arch Histol Cytol 2001;64:59–67
16. Shiota C, Larsson O, Shelton KD, et al. Sulfonylurea receptor type 1 knock-out mice have intact feeding-stimulated insulin secretion despite marked impairment in their response to glucose. J Biol Chem 2002;277:37176–37183
17. Postic C, Shiota M, Niswender KD, et al. Dual roles for glucokinase in glucose homeostasis as determined by liver and pancreatic beta cell-specific gene knock-outs using Cre recombinase. J Biol Chem 1999;274:305–315
18. Srinivas S, Watanabe T, Lin CS, et al. Cre reporter strains produced by targeted insertion of EYFP and ECFP into the ROSA26 locus. BMC Dev Biol 2001;1:4
19. Hara M, Wang X, Kawamura T, et al. Transgenic mice with green fluorescent protein-labeled pancreatic beta -cells. Am J Physiol Endocrinol Metab 2003;284:E177–E183
20. Burlison JS, Long Q, Fujitani Y, Wright CV, Magnuson MA. Pdx-1 and Ptf1a concurrently determine fate specification of pancreatic multipotent progenitor cells. Dev Biol 2008;316:74–86
21. Vierra NC, Dadi PK, Jeong I, Dickerson M, Powell DR, Jacobson DA. Type 2 diabetes-associated K+ channel TALK-1 modulates β-cell electrical excitability, second-phase insulin secretion, and glucose homeostasis. Diabetes 2015;64:3818–3828
22. Dadi PK, Vierra NC, Jacobson DA. Pancreatic β-cell-specific ablation of TASK-1 channels augments glucose-stimulated calcium entry and insulin secretion, improving glucose tolerance. Endocrinology 2014;155:3757–3768
23. Dobin A, Davis CA, Schlesinger F, et al. STAR: ultrafast universal RNA-seq aligner. Bioinformatics 2013;29:15–21
24. Anders S, Pyl PT, Huber W. HTSeq–a Python framework to work with high-throughput sequencing data. Bioinformatics 2015;31:166–169
25. Love MI, Huber W, Anders S. Moderated estimation of fold change and dispersion for RNA-seq data with DESeq2. Genome Biol 2014;15:550
26. Janky R, Verfaillie A, Imrichová H, et al. iRegulon: from a gene list to a gene regulatory network using large motif and track collections. PLoS Comput Biol 2014;10:e1003731
27. Miki T, Nagashima K, Tashiro F, et al. Defective insulin secretion and enhanced insulin action in KATP channel-deficient mice. Proc Natl Acad Sci U S A 1998;95:10402–10406
28. Seghers V, Nakazaki M, DeMayo F, Aguilar-Bryan L, Bryan J. Sur1 knockout mice. A model for K(ATP) channel-independent regulation of insulin secretion. J Biol Chem 2000;275:9270–9277
29. Düfer M, Haspel D, Krippeit-Drews P, Aguilar-Bryan L, Bryan J, Drews G. Oscillations of membrane potential and cytosolic Ca(2+) concentration in SUR1(-/-) beta cells. Diabetologia 2004;47:488–498
30. Nenquin M, Szollosi A, Aguilar-Bryan L, Bryan J, Henquin JC. Both triggering and amplifying pathways contribute to fuel-induced insulin secretion in the absence of sulfonylurea receptor-1 in pancreatic beta-cells. J Biol Chem 2004;279:32316–32324
31. De León DD, Li C, Delson MI, Matschinsky FM, Stanley CA, Stoffers DA. Exendin-(9-39) corrects fasting hypoglycemia in SUR-1-/- mice by lowering cAMP in pancreatic beta-cells and inhibiting insulin secretion. J Biol Chem 2008;283:25786–25793
32. Talchai C, Xuan S, Lin HV, Sussel L, Accili D. Pancreatic β cell dedifferentiation as a mechanism of diabetic β cell failure. Cell 2012;150:1223–1234
33. Brouwers B, de Faudeur G, Osipovich AB, et al. Impaired islet function in commonly used transgenic mouse lines due to human growth hormone minigene expression. Cell Metab 2014;20:979–990
34. Kanazawa Y, Makino M, Morishima Y, Yamada K, Nabeshima T, Shirasaki Y. Degradation of PEP-19, a calmodulin-binding protein, by calpain is implicated in neuronal cell death induced by intracellular Ca2+ overload. Neuroscience 2008;154:473–481
35. Kim-Muller JY, Fan J, Kim YJ, et al. Aldehyde dehydrogenase 1a3 defines a subset of failing pancreatic β cells in diabetic mice. Nat Commun 2016;7:12631
36. Okazaki K, Niki I, Iino S, Kobayashi S, Hidaka H. A role of calcyclin, a Ca(2+)-binding protein, on the Ca(2+)-dependent insulin release from the pancreatic beta cell. J Biol Chem 1994;269:6149–6152
37. Fadista J, Vikman P, Laakso EO, et al. Global genomic and transcriptomic analysis of human pancreatic islets reveals novel genes influencing glucose metabolism. Proc Natl Acad Sci U S A 2014;111:13924–13929
38. Castro DS, Martynoga B, Parras C, et al. A novel function of the proneural factor Ascl1 in progenitor proliferation identified by genome-wide characterization of its targets. Genes Dev 2011;25:930–945
39. Webb AE, Pollina EA, Vierbuchen T, et al. FOXO3 shares common targets with ASCL1 genome-wide and inhibits ASCL1-dependent neurogenesis. Cell Reports 2013;4:477–491
40. Raposo AA, Vasconcelos FF, Drechsel D, et al. Ascl1 coordinately regulates gene expression and the chromatin landscape during neurogenesis. Cell Reports 2015; 9:1544–1556
41. Mourad NI, Nenquin M, Henquin JC. Metabolic amplification of insulin secretion by glucose is independent of β-cell microtubules. Am J Physiol Cell Physiol 2011; 300:C697–C706
42. Kligman D, Hilt DC. The S100 protein family. Trends Biochem Sci 1988;13:437–443
43. Mellström B, Savignac M, Gomez-Villafuertes R, Naranjo JR. Ca2+-operated transcriptional networks: molecular mechanisms and in vivo models. Physiol Rev 2008;88:421–449
44. Udovichenko IP, Gibbs D, Williams DS. Actin-based motor properties of native myosin VIIa. J Cell Sci 2002;115:445–450
45. Wang Z, York NW, Nichols CG, Remedi MS. Pancreatic β cell dedifferentiation in diabetes and redifferentiation following insulin therapy. Cell Metab 2014;19:872–882
46. Brereton MF, Iberl M, Shimomura K, et al. Reversible changes in pancreatic islet structure and function produced by elevated blood glucose. Nat Commun 2014;5:4639
47. Segerstolpe Å, Palasantza A, Eliasson P, et al. Single-cell transcriptome profiling of human pancreatic islets in health and type 2 diabetes. Cell Metab 2016;24:593–607
48. Xin Y, Kim J, Okamoto H, et al. RNA sequencing of single human islet cells reveals type 2 diabetes genes. Cell Metab 2016;24:608–615

49. Giannone G, Rondé P, Gaire M, et al. Calcium rises locally trigger focal adhesion disassembly and enhance residency of focal adhesion kinase at focal adhesions. J Biol Chem 2004;279:28715–28723
50. Pang ZP, Yang N, Vierbuchen T, et al. Induction of human neuronal cells by defined transcription factors. Nature 2011;476:220–223
51. Brun PJ, Grijalva A, Rausch R, et al. Retinoic acid receptor signaling is required to maintain glucose-stimulated insulin secretion and β-cell mass. FASEB J 2015;29: 671–683
52. Lu M, Seufert J, Habener JF. Pancreatic beta-cell-specific repression of insulin gene transcription by CCAAT/enhancer-binding protein beta. Inhibitory interactions with basic helix-loop-helix transcription factor E47. J Biol Chem 1997;272:28349–28359
53. Matsuda T, Kido Y, Asahara S, et al. Ablation of C/EBPbeta alleviates ER stress and pancreatic beta cell failure through the GRP78 chaperone in mice. J Clin Invest 2010;120:115–126
54. Moutier E, Ye T, Choukrallah MA, et al. Retinoic acid receptors recognize the mouse genome through binding elements with diverse spacing and topology. J Biol Chem 2012;287:26328–26341
55. Thompson M, Andrade VA, Andrade SJ, et al. Inhibition of the TEF/TEAD transcription factor activity by nuclear calcium and distinct kinase pathways. Biochem Biophys Res Commun 2003;301:267–274
56. Pontoglio M, Sreenan S, Roe M, et al. Defective insulin secretion in hepatocyte nuclear factor 1alpha-deficient mice. J Clin Invest 1998;101:2215–2222